

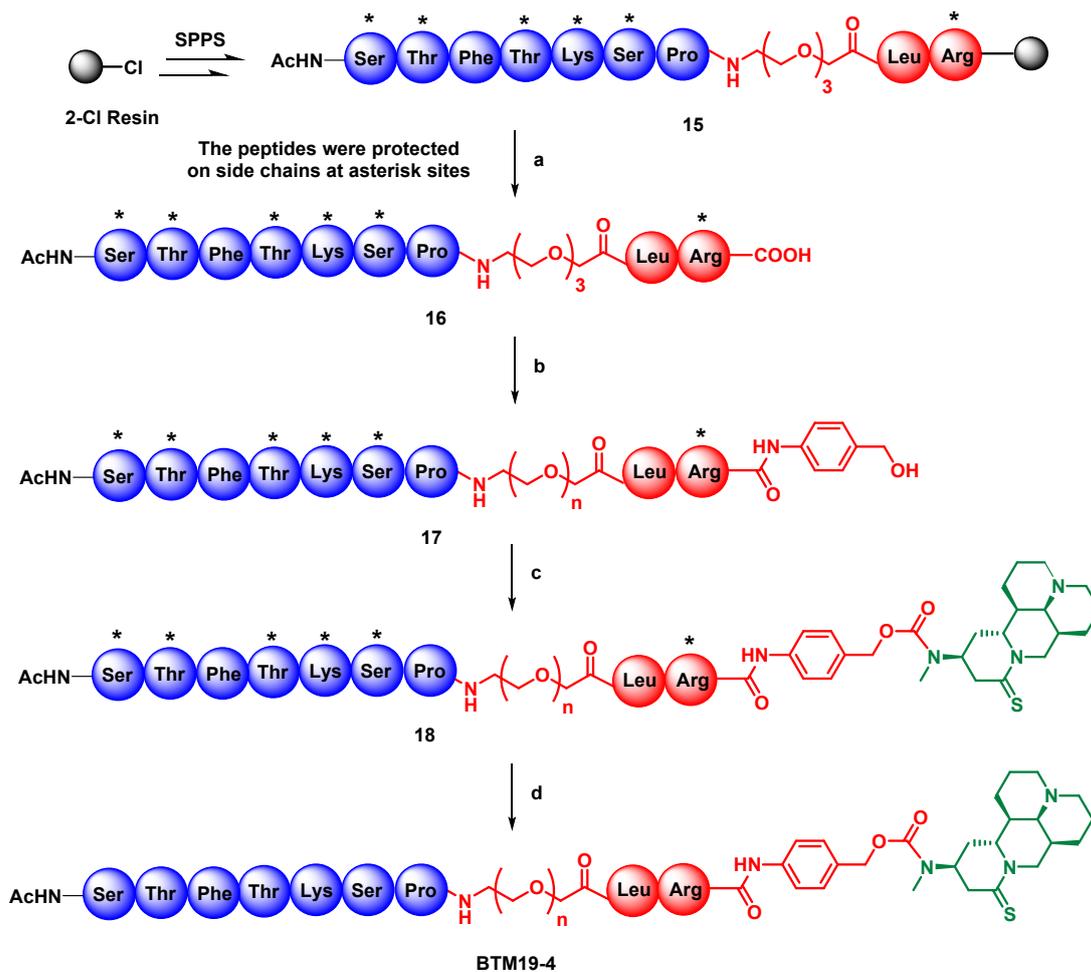
Supporting Information

Development of Novel Bone Targeting Peptide-Drug Conjugate of 13-aminomethyl-15-thiomatine for Osteoporosis Therapy

Jia Su^{a†}, Chao Liu^{b†}, Haohao Bai^b, Wei Cong^b, Hua Tang^b, Honggang Hu^b, Li Su^{b*}, Shipeng He^{b*}
and Yong Wang^{a*}

^a *Department of Orthopaedics, Wenzhou Hospital of Integrated Traditional Chinese and Western Medicine, Zhejiang, China.*

^b *Institute of Translational Medicine, Shanghai University, Shanghai, China.*



Scheme S1. The synthesis route of **BTM19-4**. Reagents and conditions: a) TFE/DCM (1:3, v/v), rt, 4 h, 87%; b) 4-aminophenyl methanol, HOBT, DIC, DMF, rt, 2 h, 74%; c) i) Triphosgene, activated carbon, THF, rt, 12 h; ii) **M19**, Et₃N, DMF, rt, 12 h, 76% in two steps; d) TFA/water/EDT/TIPs (95:2:2:1, v/v/v/v), rt, 2 h, 59%.

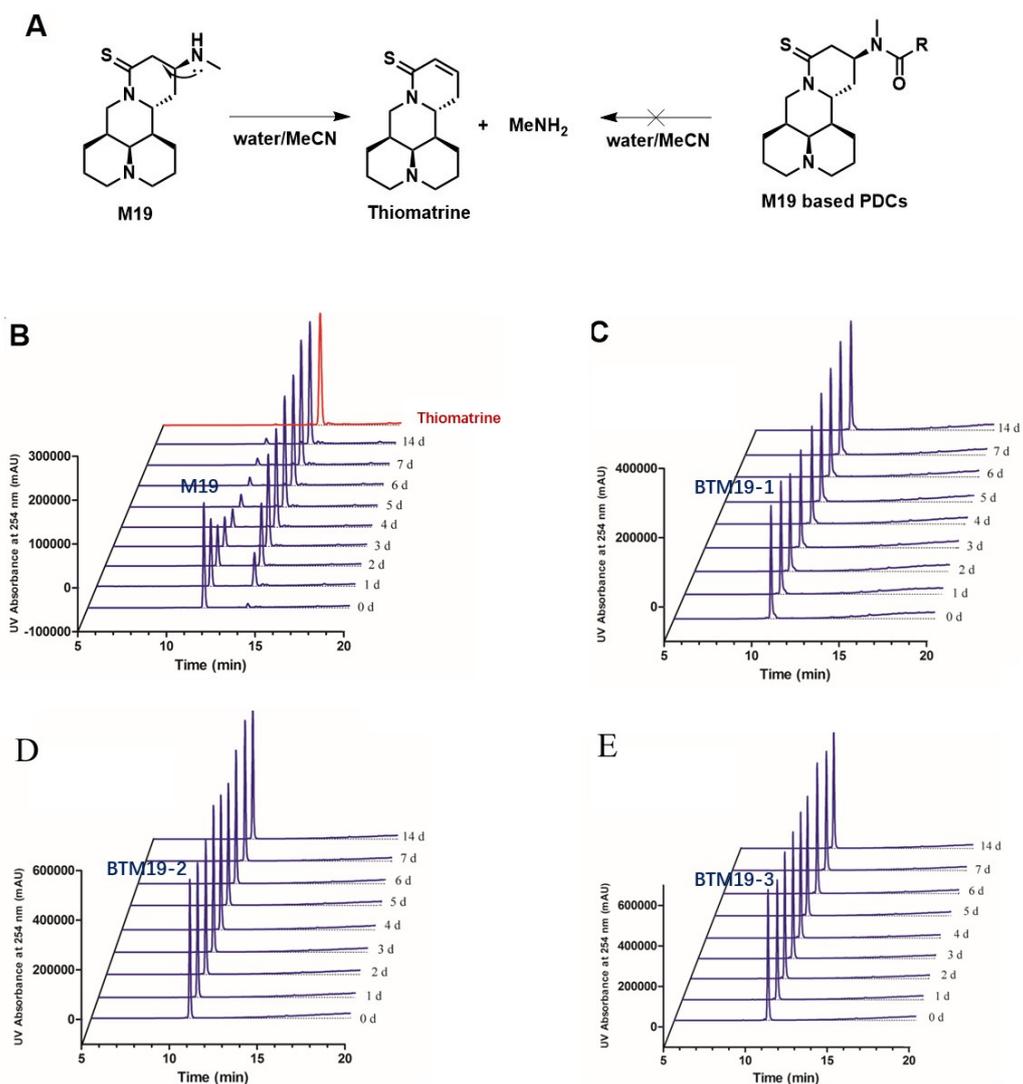


Figure S1. (A) Illustration of the chemical stability study of M19 vs. PDCs in water/MeCN solution at room temperature; Chromatograms of chemical stability study of M19 (B), BTM19-1 (C), BTM19-2 (D), BTM19-3 (E).

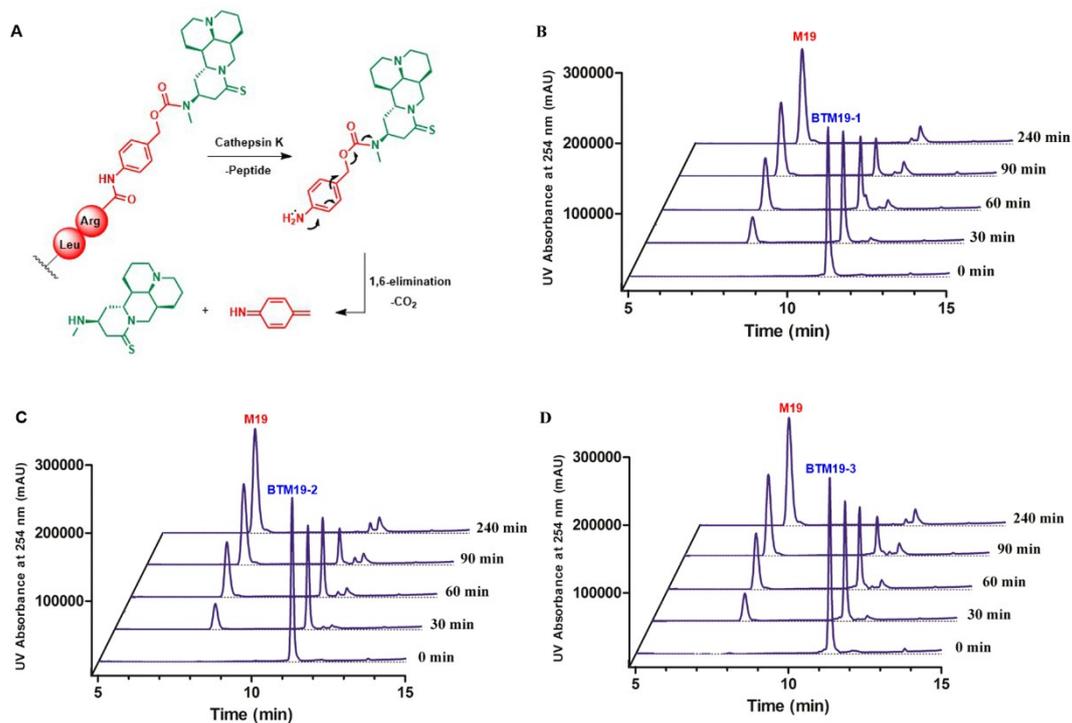


Figure S2. (A) Mechanism of the drug release from self-immolative spacer PABC and Cathepsin K substrate; Chromatograms of drug release study of **BTM19-1** (B), **BTM19-2** (C) and **BTM19-3** (D) at pH 5.5 (37 °C) with cathepsin K.

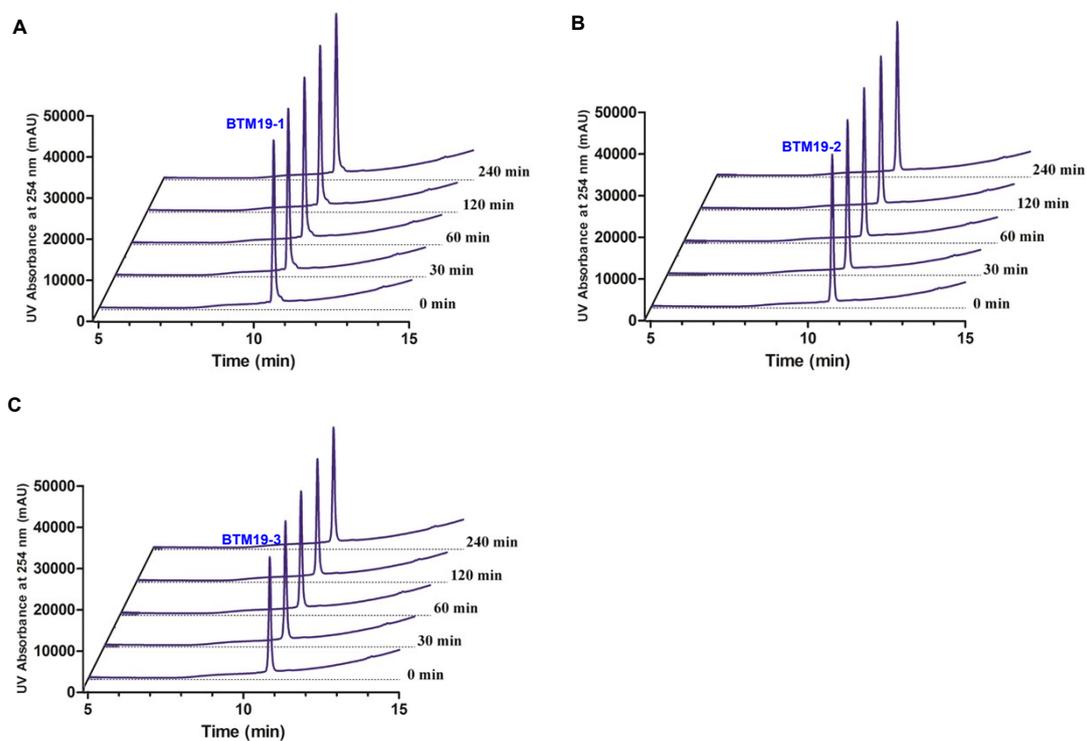


Figure S3. Chromatograms of proteolytic stability study of **BTM19-1** (A), **BTM19-2** (B), **BTM19-3** (C) under α -chymotrypsin treatment.

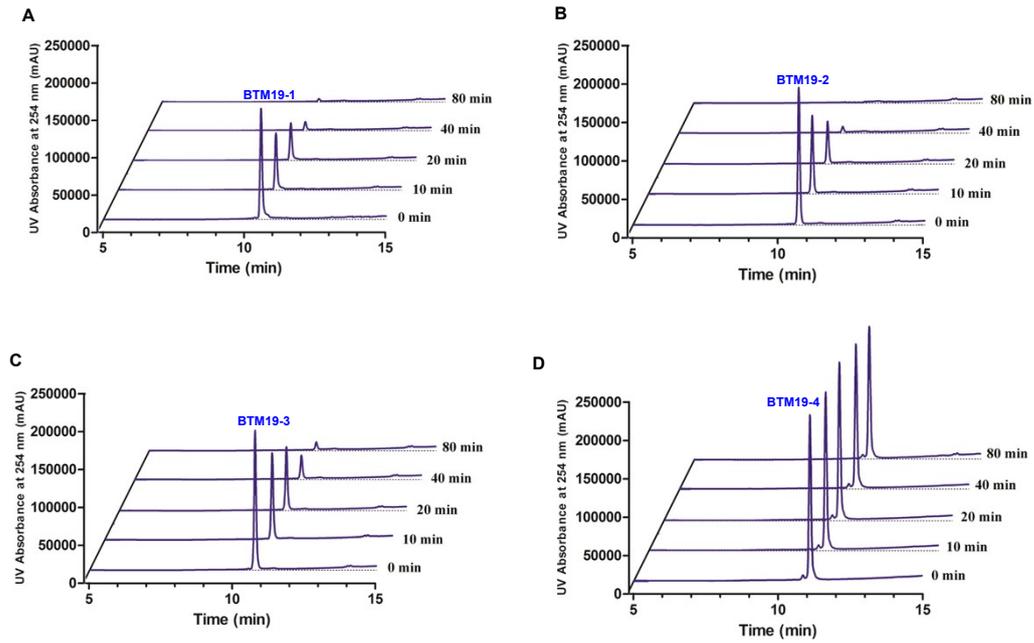


Figure S4. Chromatograms of binding study of **BTM19-1** (A), **BTM19-2** (B), **BTM19-3** (C) and **BTM19-4** (D) to hydroxyapatite at pH=5.5 and 37 °C.

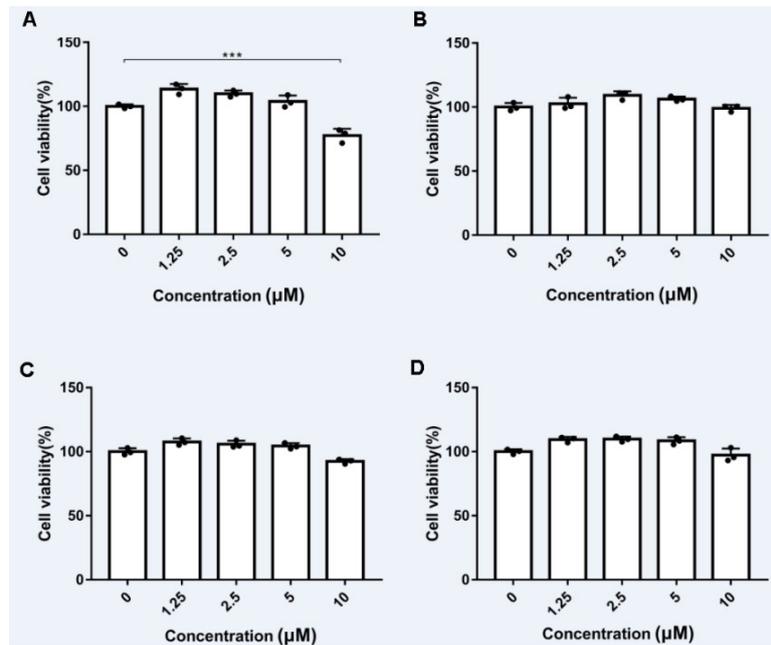


Figure S5. Quantification data of cytotoxic study after **M19** (A), **BTM19-1** (B), **BTM19-2** (C) and **BTM19-3** (D) treatment on RAW264.7 cell measured by CCK-8 assay. Data points are displayed as the mean value SEM of duplicate independent experiments. (* $P < 0.05$, ** $P < 0.01$, *** $P < 0.001$).

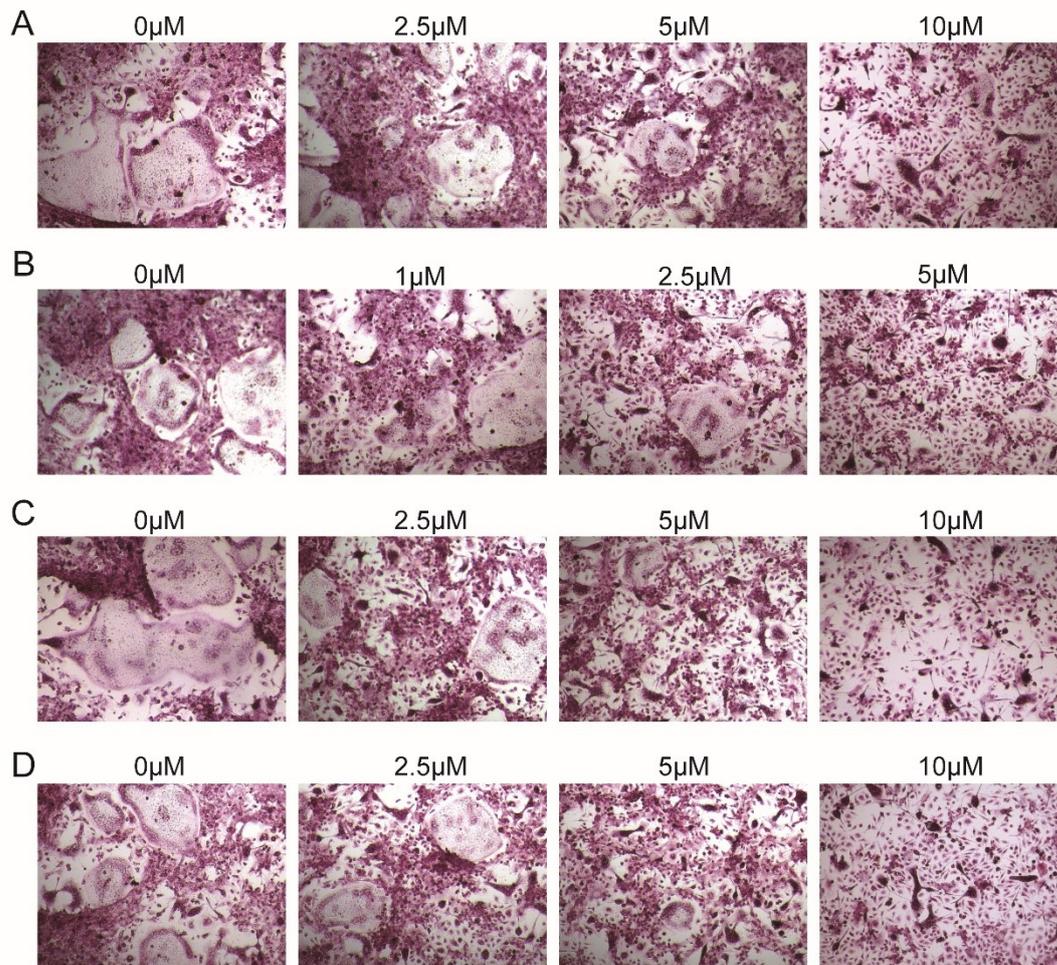


Figure S6. Formation of TRAP-positive cells from RAW264.7 cells with RANKL, M-CSF and treated with **M19** (A), **BTM19-1** (B), **BTM19-2** (C) and **BTM19-3** (D).

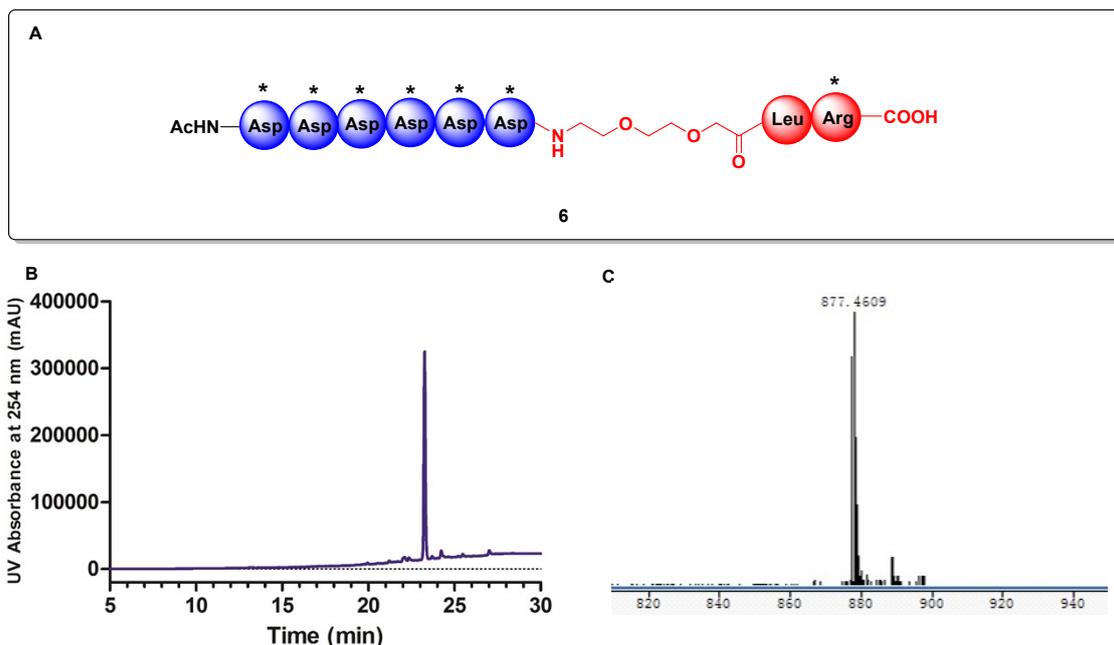


Figure S7. **6** as white powder, 1.43 g, 82% yield. **A)** Structure of **BTM19-1-2**; **B)** HPLC trace of purified **BTM19-1-2**. Gradient: 90-0% of buffer B in 20 min with C18 column (5 μ m, 2.5 mm \times 250 mm). **C)** HR-MS spectrum of **BTM19-1-2** (calcd. for $C_{81}H_{132}N_{12}O_{28}S$ 1752.8995; found $[M+2H]^{2+}$ 877.4609).

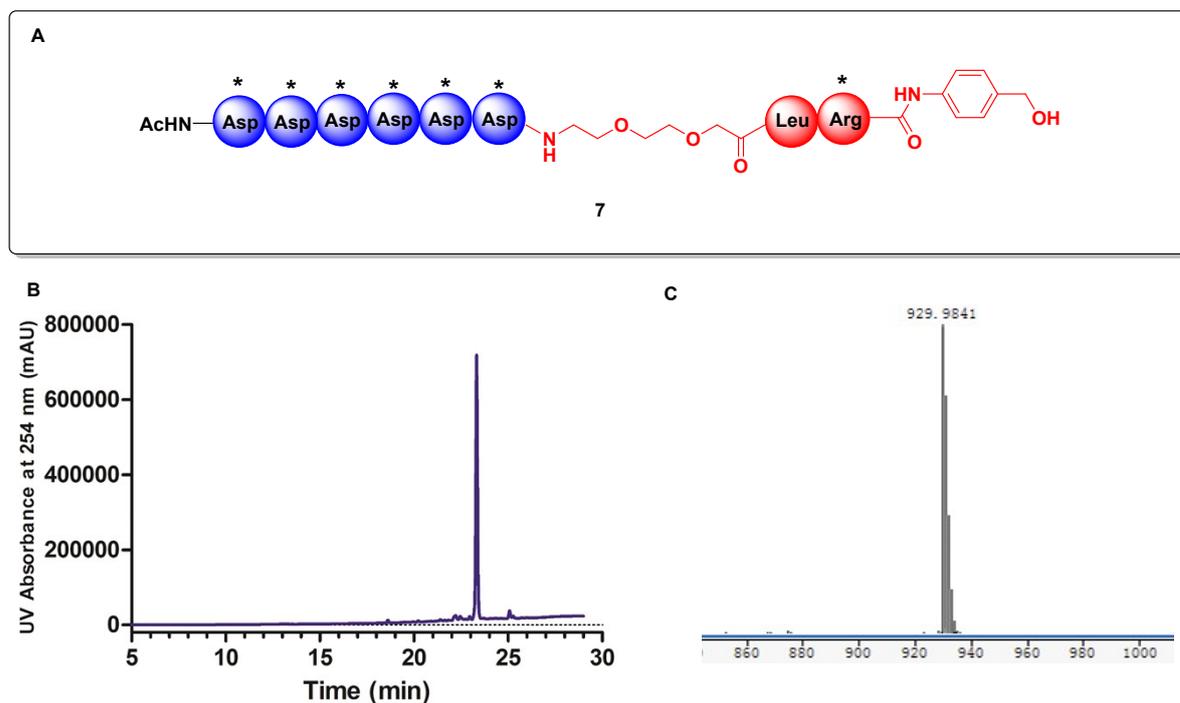


Figure S8. **7** as white powder, 1.12 g, 79% yield. **A)** Structure of **BTM19-1-3**; **B)** HPLC trace of purified **BTM19-1-3**. Gradient: 90-0% of buffer B in 20 min with C18 column (5 μ m, 2.5 mm \times 250 mm). **C)** HR-MS spectrum of **BTM19-1-3** (calcd. for $C_{88}H_{139}N_{13}O_{28}S$ 1857.9573; found $[M+2H]^{2+}$ 929.9841).

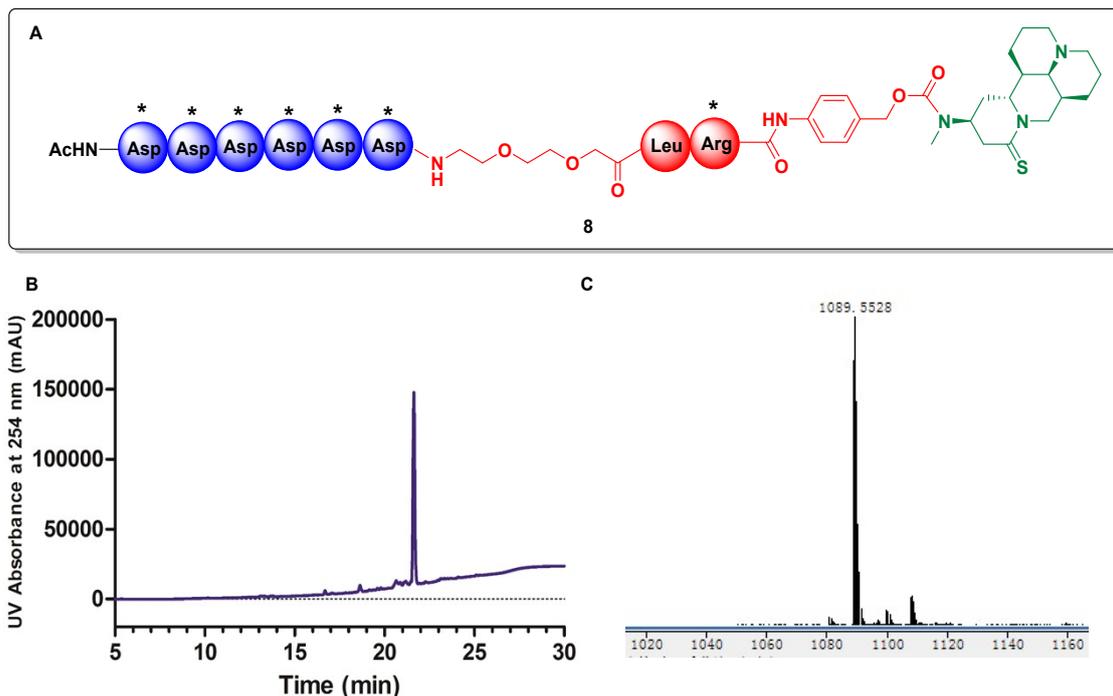


Figure S9. **8** as white powder, 1.1 g, 78% yield. **A)** Structure of **BTM19-1-4**; **B)** HPLC trace of purified **BTM19-1-4**. Gradient: 90-0% of buffer B in 20 min with C18 column (5 μ m, 2.5 mm \times 250 mm). **C)** HR-MS spectrum of **BTM19-1-4** (calcd. for C₁₀₅H₁₆₄N₁₆O₂₉S₂ 2177.1292; found [M+2H]²⁺ 1089.5528).

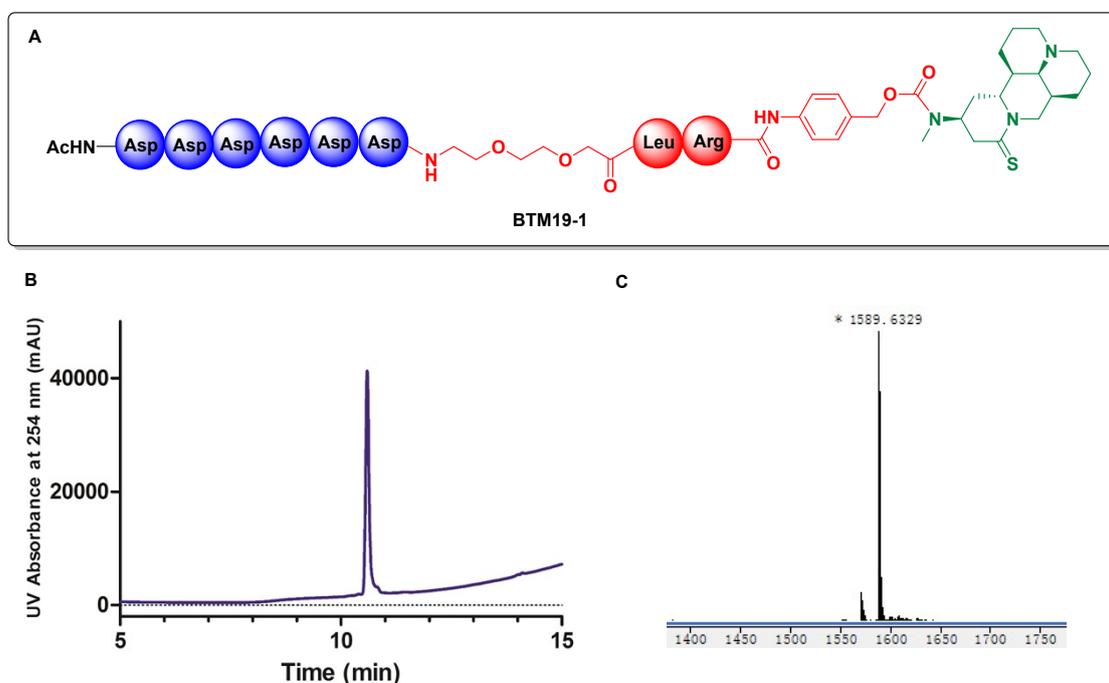


Figure S10. **BTM19-1** as lyophilized white powder, 492 mg, 62% yield. **A)** Structure of **BTM19-1**; **B)** HPLC trace of purified **BTM19-1**. Gradient: 90-0% of buffer B in 15 min with C18 column (5 μ m, 2.5 mm \times 250 mm). **C)** HR-MS spectrum of **BTM19-**

1 (calcd. for $C_{68}H_{100}N_{16}O_{26}S$ 1588.6715; found $[M+H]^+$ 1589.6329).

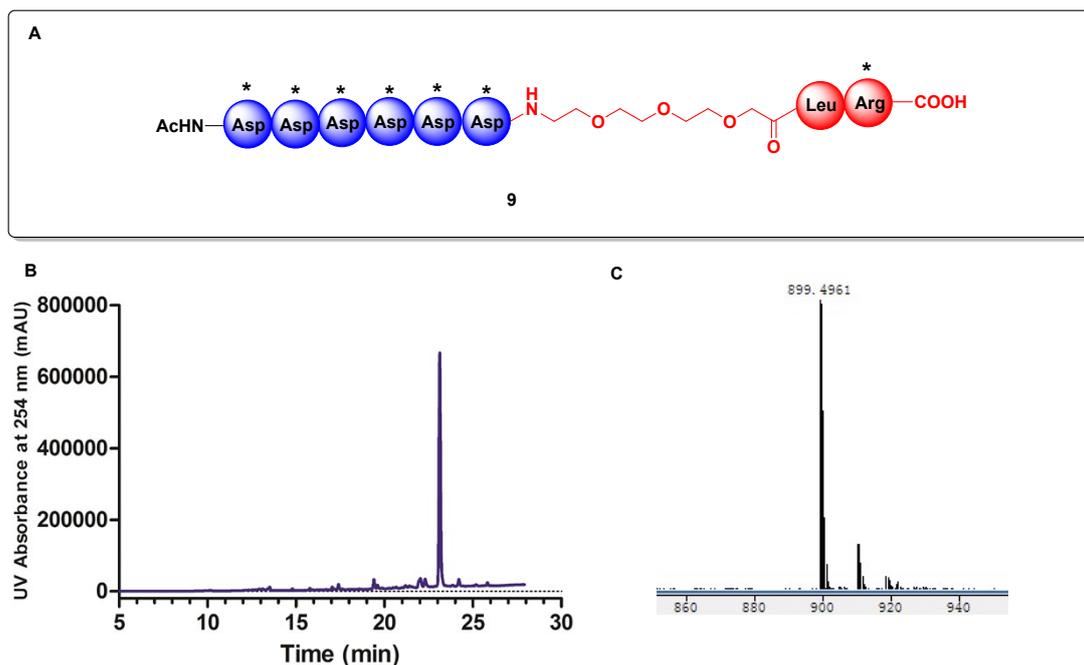


Figure S11. **9** as white powder, 1.5 g, 83% yield. **A)** Structure of **BTM19-2-2**; **B)** HPLC trace of purified **BTM19-2-2**. Gradient: 90-0% of buffer B in 20 min with C18 column ($5\ \mu\text{m}$, $2.5\ \text{mm}\times 250\ \text{mm}$). **C)** HR-MS spectrum of **BTM19-2-2** (calcd. for $C_{83}H_{136}N_{12}O_{29}S$ 1796.9257; found $[M+2H]^{2+}$ 899.4961).

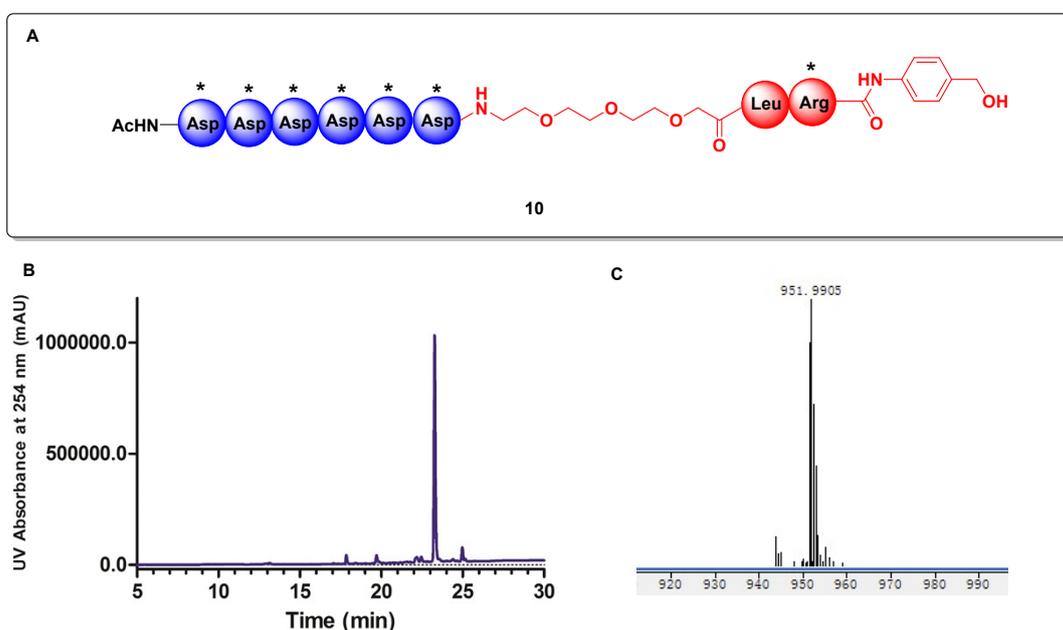


Figure S12. **10** as white powder, 1.18 g, 75% yield. **A)** Structure of **BTM19-2-3**; **B)** HPLC trace of purified **BTM19-2-3**. Gradient: 90-0% of buffer B in 20 min with C18 column ($5\ \mu\text{m}$, $2.5\ \text{mm}\times 250\ \text{mm}$). **C)** HR-MS spectrum of **BTM19-2-3** (calcd. for $C_{90}H_{143}N_{13}O_{29}S$ 1901.9835; found $[M+2H]^{2+}$ 951.9905).

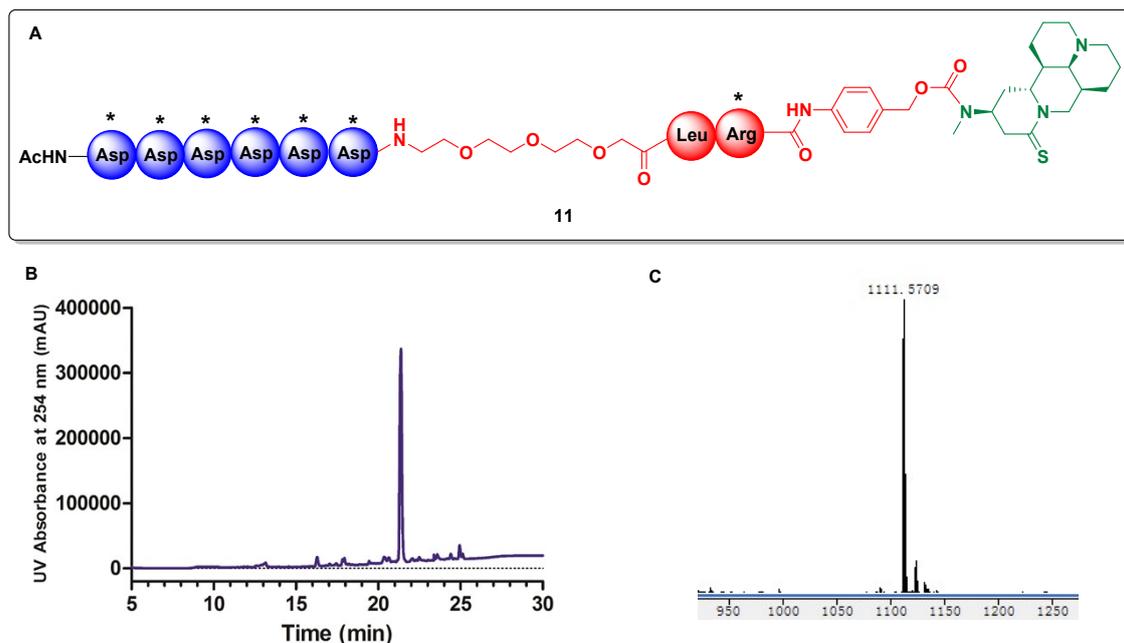


Figure S13. **11** as white powder, 1.07 g, 85% yield. **A)** Structure of **BTM19-2-4**; **B)** HPLC trace of purified **BTM19-2-4**. Gradient: 90-0% of buffer B in 20 min with C18 column (5 μ m, 2.5 mm \times 250 mm). **C)** HR-MS spectrum of **BTM19-2-4** (calcd. for $C_{107}H_{168}N_{16}O_{30}S_2$ 2221.1554; found $[M+2H]^{2+}$ 1111.5709).

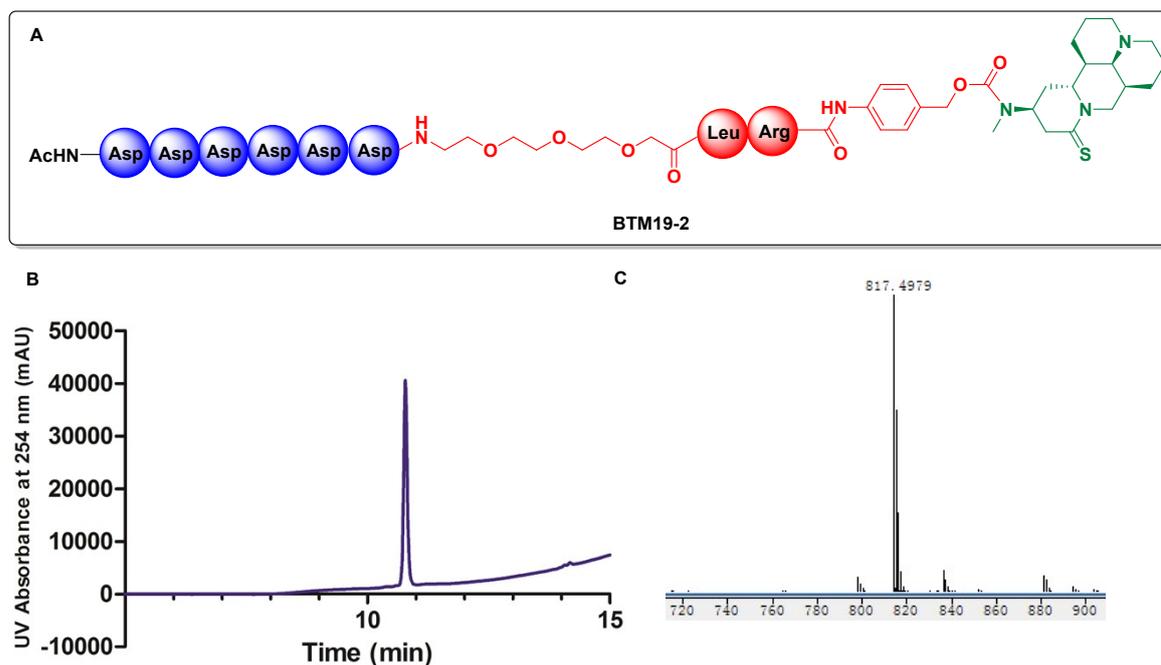


Figure S14. **BTM19-2** as lyophilized white powder, 493 mg, 63% yield. **A)** Structure of **BTM19-2**; **B)** HPLC trace of purified **BTM19-2**. Gradient: 90-0% of buffer B in 15 min with C18 column (5 μ m, 2.5 mm \times 250 mm). **C)** HR-MS spectrum of **BTM19-2** (calcd. for $C_{70}H_{104}N_{16}O_{27}S$ 1632.9678; found $[M+2H]^{2+}$ 817.4979).

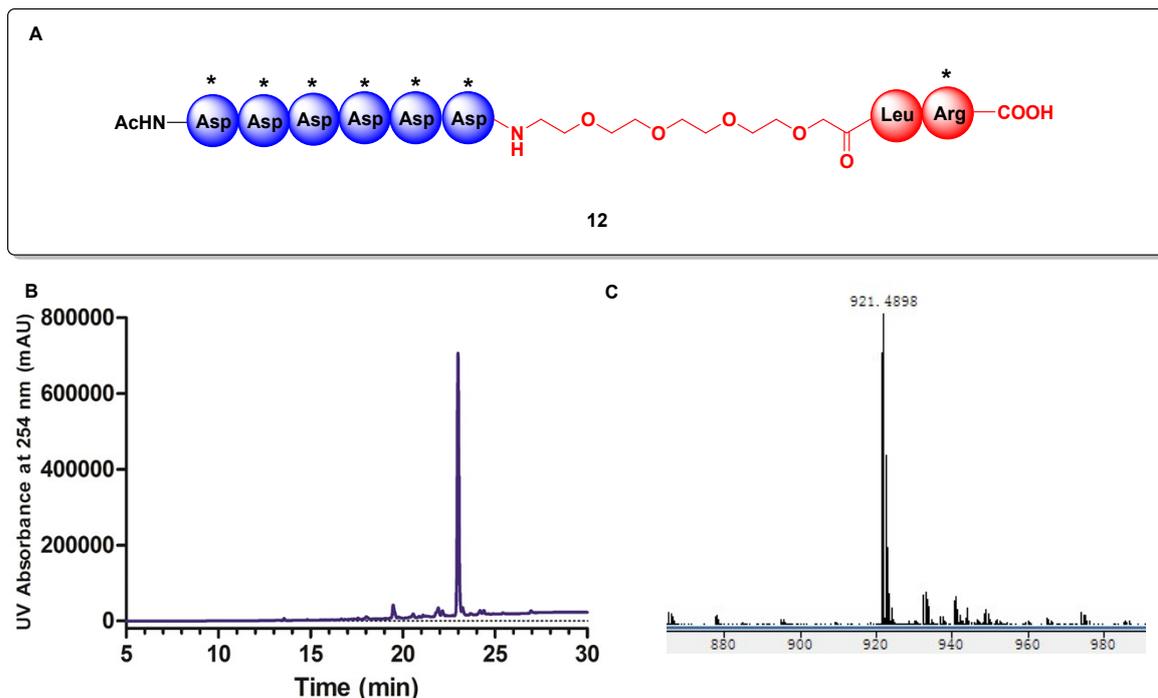


Figure S15. **12** as white powder, 1.47 g, 80% yield. **A)** Structure of **BTM19-3-2**; **B)** HPLC trace of purified **BTM19-3-2**. Gradient: 90-0% of buffer B in 20 min with C18 column (5 μ m, 2.5 mm \times 250 mm). **C)** HR-MS spectrum of **BTM19-3-2** (calcd. for $C_{85}H_{140}N_{12}O_{30}S$ 1840.9519; found $[M+2H]^{2+}$ 921.4898).

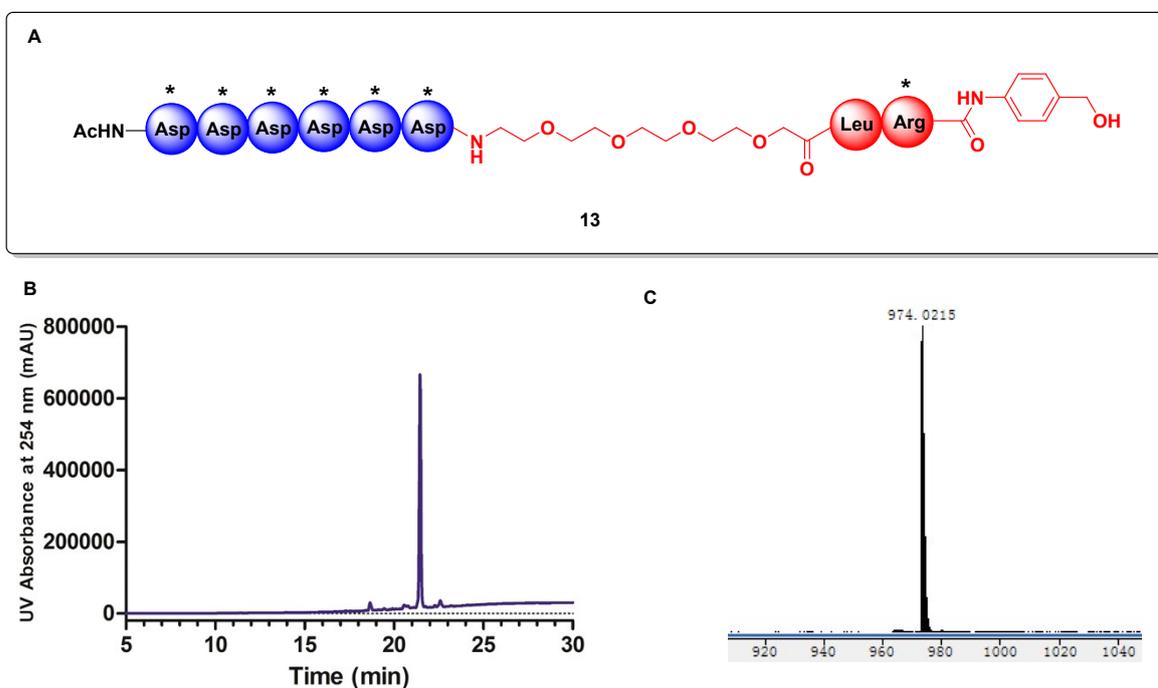


Figure S16. **13** as white powder, 1.15 g, 74% yield. **A)** Structure of **BTM19-3-3**; **B)** HPLC trace of purified **BTM19-3-3**. Gradient: 90-0% of buffer B in 20 min with C18 column (5 μ m, 2.5 mm \times 250 mm). **C)** HR-MS spectrum of **BTM19-3-3** (calcd. for $C_{92}H_{147}N_{13}O_{30}S$ 1946.0098; found $[M+2H]^{2+}$ 974.0215).

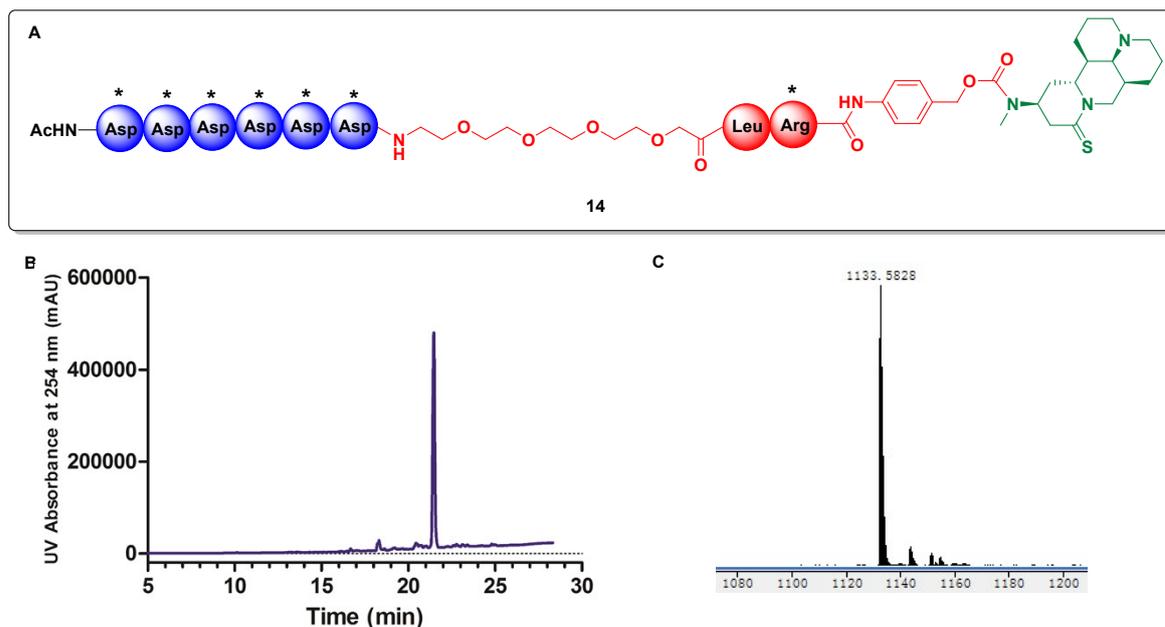


Figure S17. **14** as white powder 1.09 g, 86% yield. **A)** Structure of **BTM19-3-4**; **B)** HPLC trace of purified **BTM19-3-4**. Gradient: 90-0% of buffer B in 20 min with C18 column (5 μ m, 2.5 mm \times 250 mm). **C)** HR-MS spectrum of **BTM19-3-4** (calcd. for $C_{109}H_{172}N_{16}O_{31}S_2$ 2265.1816; found $[M+2H]^{2+}$ 1133.5828).

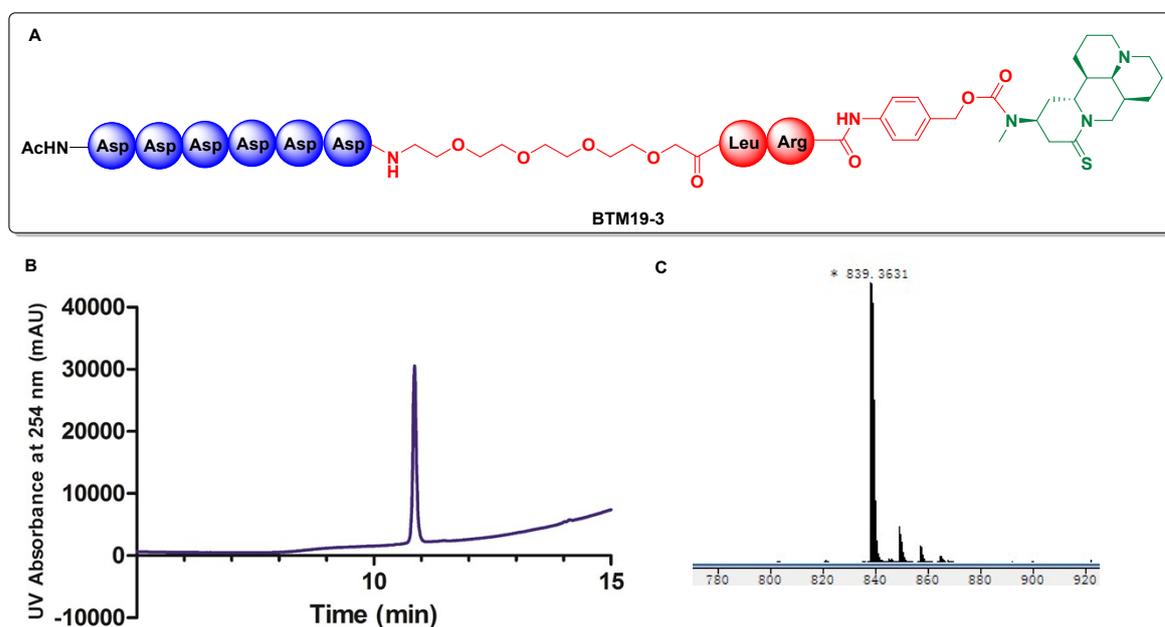


Figure S18. **BTM19-3** as lyophilized white powder, 443 mg, 60% yield. **A)** Structure of **BTM19-3**; **B)** HPLC trace of purified **BTM19-3**. Gradient: 90-0% of buffer B in 15 min with C18 column (5 μ m, 2.5 mm \times 250 mm). **C)** HR-MS spectrum of **BTM19-3** (calcd. for $C_{72}H_{108}N_{16}O_{28}S$ 1676.7240; found $[M+2H]^{2+}$ 839.3631).

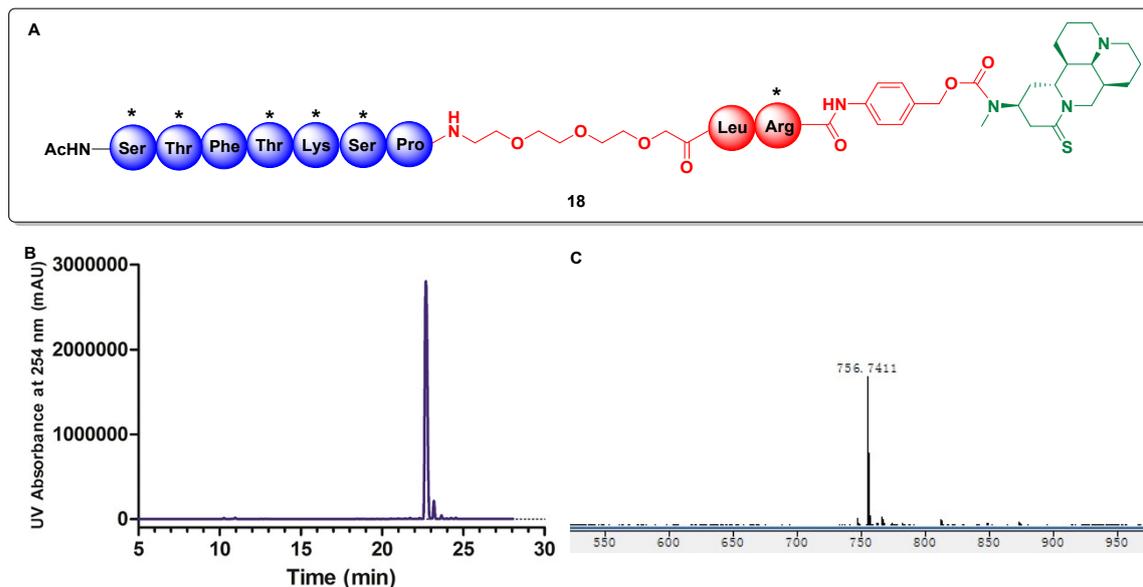


Figure S21. **18** as white powder, 1.05 g, 76% yield. **A)** Structure of **BTM19-4-4**; **B)** HPLC trace of purified **BTM19-4-4**. Gradient: 90-0% of buffer B in 20 min with C18 column (5 μ m, 2.5 mm \times 250 mm). **C)** HR-MS spectrum of **BTM19-4-4** (calcd. for $C_{114}H_{182}N_{18}O_{25}S_2$ 2267.2965; found $[M+3H]^{3+}$ 756.7441).

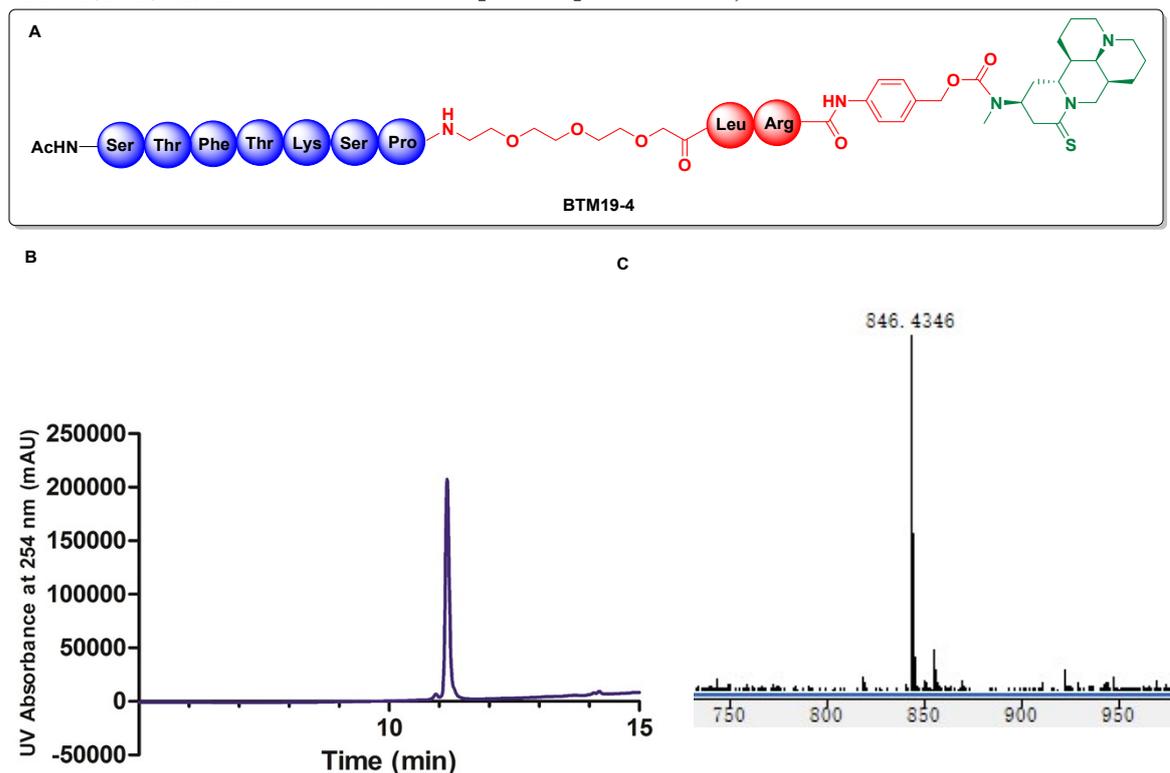


Figure S22. **BTM19-4** as lyophilized white powder, 458 mg, 59% yield. **A)** Structure of **BTM19-4**; **B)** HPLC trace of purified **BTM19-4**. Gradient: 90-0% of buffer B in 15 min with C18 column (5 μ m, 2.5 mm \times 250 mm). **C)** HR-MS spectrum of **BTM19-4** (calcd. for $C_{80}H_{126}N_{18}O_{20}S$ 1690.9116; found $[M+2H]^{2+}$ 846.4346).

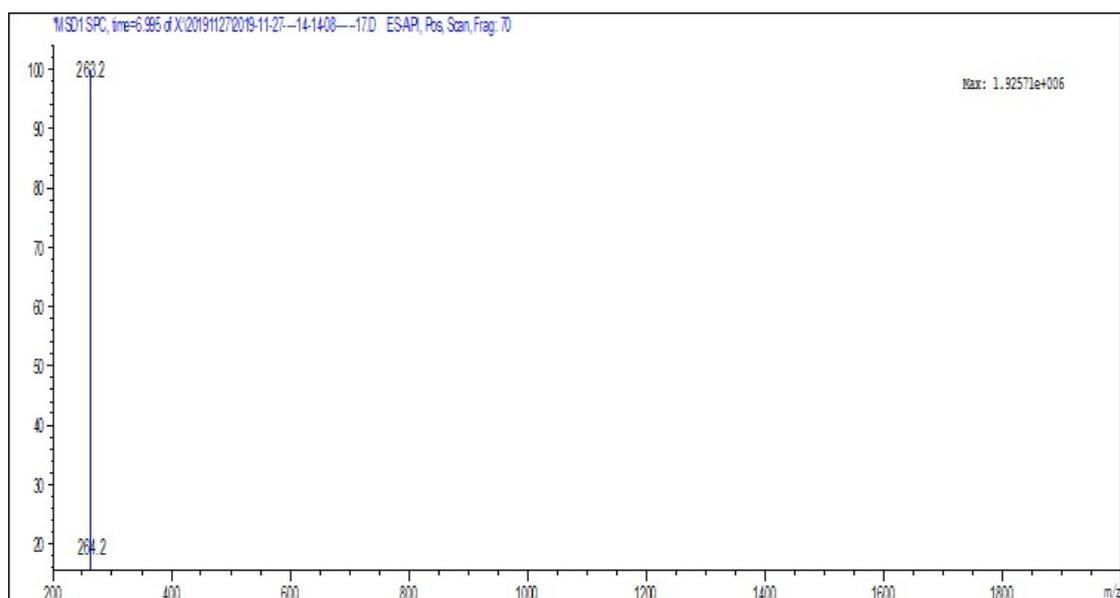


Figure S23. ESI-MS spectrum of **2** (calculated for $C_{15}H_{22}N_2S$ 262.15; found $[M+H]^+$ 263.2).

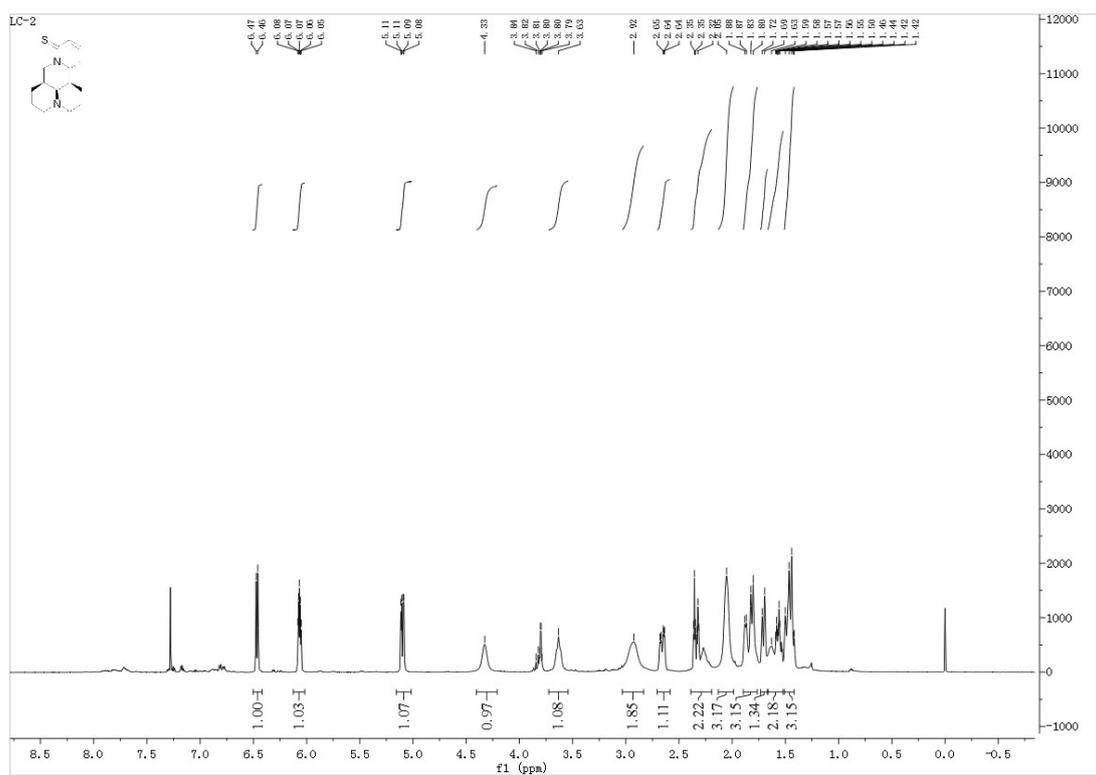


Figure S24. 1H -NMR data of **2**.

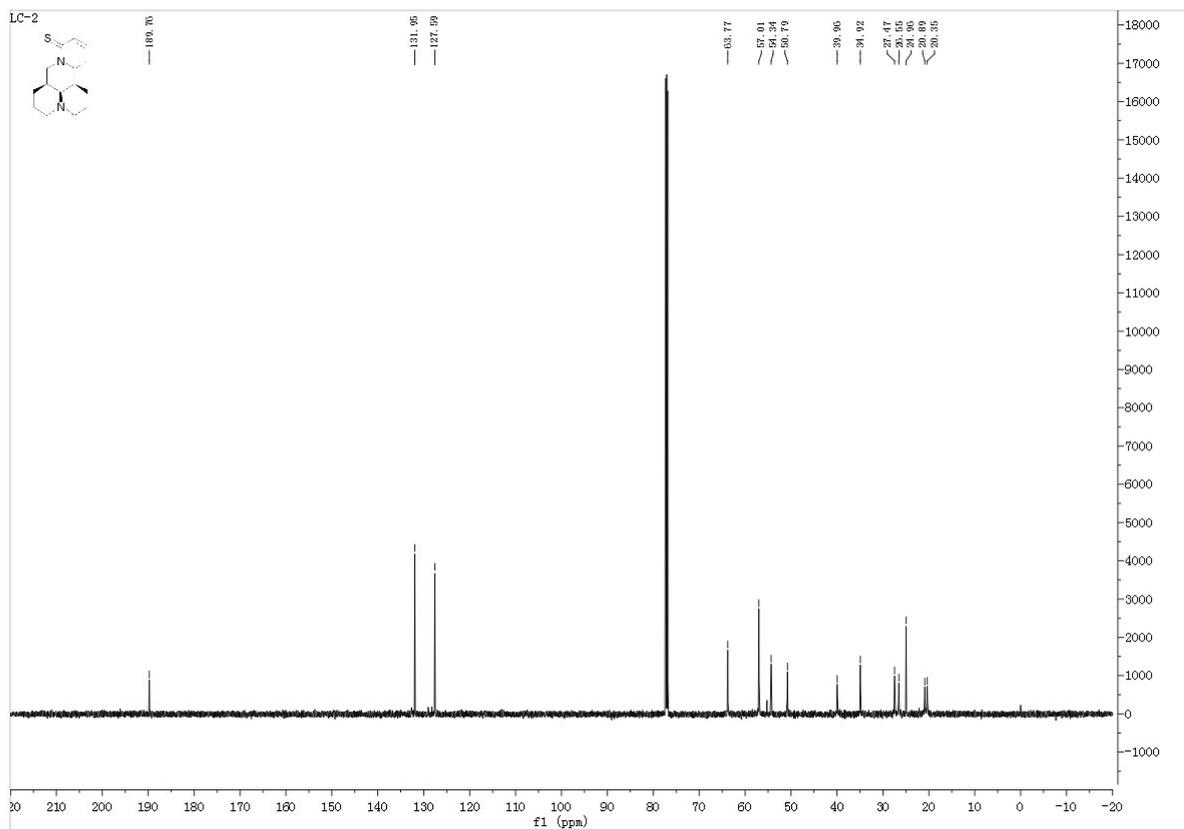


Figure S25. ^{13}C -NMR data of **2**.

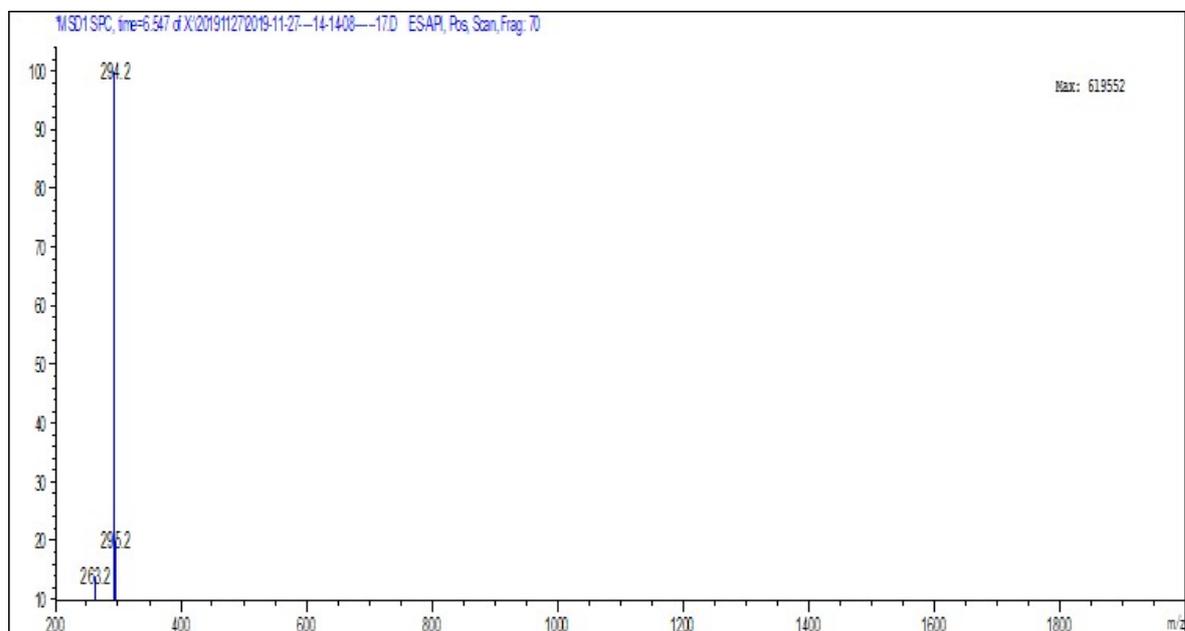


Figure S26. ESI-MS spectrum of **3** (calculated for $\text{C}_{16}\text{H}_{27}\text{N}_3\text{S}$ 293.19; found $[\text{M}+\text{H}]^+$ 294.2).

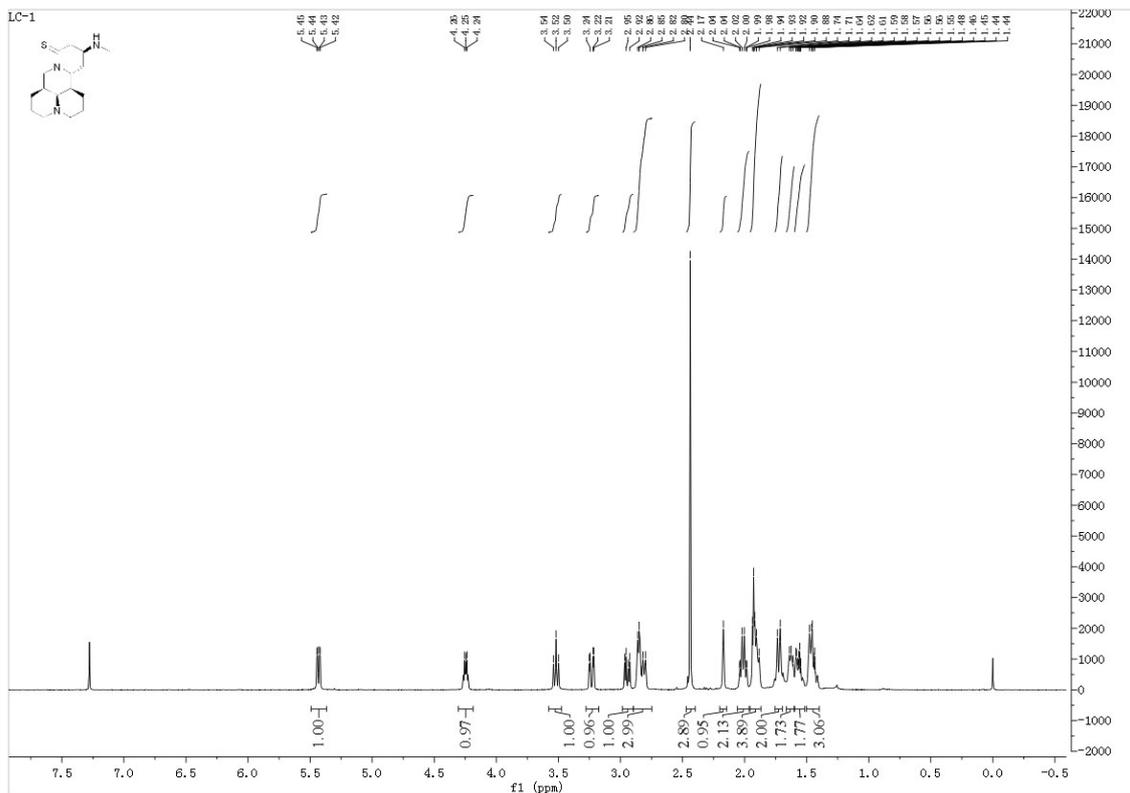


Figure S27. ^1H -NMR data of **2**.

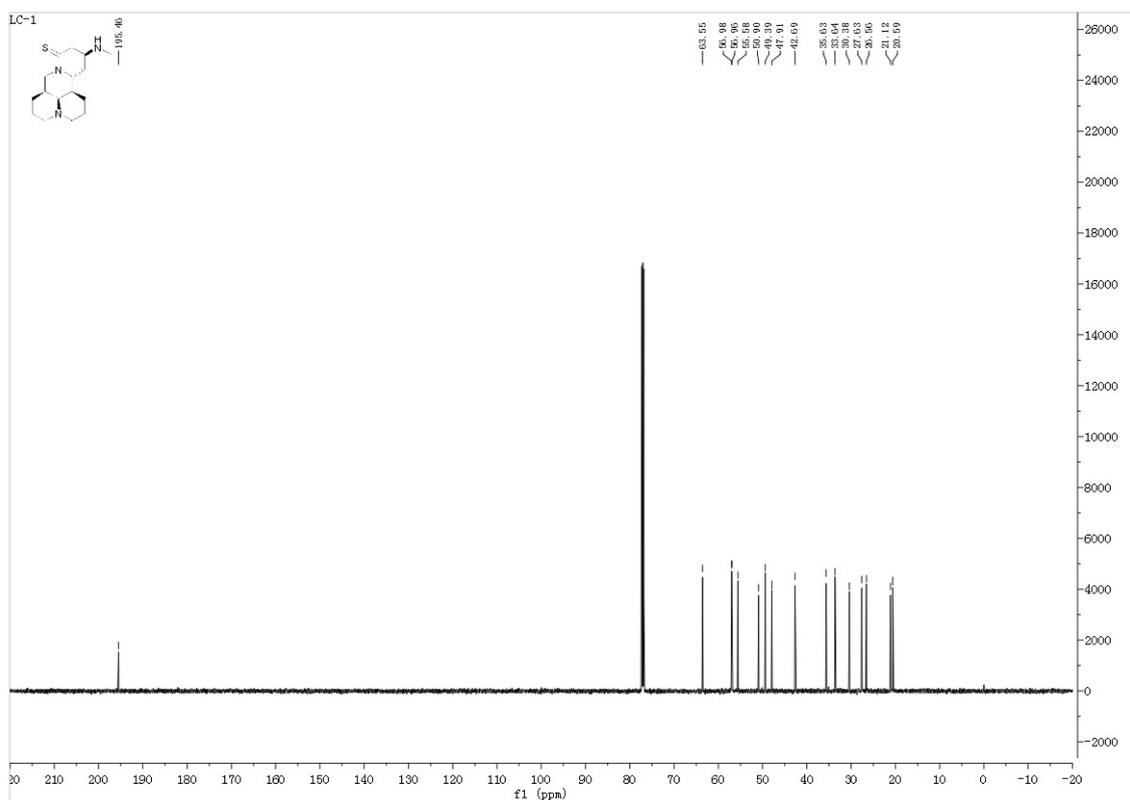


Figure S28. ^{13}C -NMR data of **2**.